In Vivo and *in Vitro* ^{31}P Magnetic Resonance Spectroscopic Studies of the Hepatic Response of Healthy Rats and Rats with Acute Hepatic Damage to Fructose Loading

Wuhua Lu, Steven J. Locke, Manfred Brauer

The hepatic response to a fructose challenge for control rats, and rats subjected to an acute sublethal dose of carbon tetrachloride (CCl_4) or bromobenzene (BB), was compared using dynamic *in vivo* ^{31}P MRS. Fructose loading conditions were used in which control rats showed only a modest increase in hepatic phosphomonoester (PME), and a small decrease in ATP, P_i, and intracellular pH after fructose administration. Both CCl_4 and BB-treated rats showed a much greater fructose-induced accumulation of PME than did controls. Trolox C, a free radical scavenger, prevented most of this PME increase. BB-treated rats, given sufficient time to recover from the hepatotoxic insult, responded to the fructose load similarly to controls. Liver aldolase activities of control, toxicant-treated rats, and toxicant plus Trolox C-treated rats correlated inversely with PME accumulation after fructose loading (correlation coefficient: −0.834, $P < 0.05$). Perchloric acid extracts of rat livers studied by *in vitro* ^{31}P MRS confirmed that the PME accumulation after fructose loading is mainly due to an increase in fructose 1-phosphate. These studies are consistent with the aldolase-catalyzed cleavage of fructose 1-phosphate being rate-limiting in hepatic fructose metabolism, and that the CCl_4 and BB treatment modify and inactivate the aldolase enzyme.

Key words: ^{31}P magnetic resonance spectroscopy; fructose; hepatotoxicants; aldolase.

INTRODUCTION

In vivo ^{31}P magnetic resonance spectroscopy (MRS) is now a well-established research technique for noninvasive detection of metabolites such as adenosine triphosphate (ATP), phosphocreatine (PCr), inorganic phosphate (P_i), phosphomonoesters (PME), and phosphodiesters (PDE) within an organ *in situ* (1–5). The method has the unique advantage of monitoring dynamic changes in these phosphorus-containing tissue metabolites as a function of time, such as during the hepatic metabolism of a fructose load within an intact animal. Fructose is metabolized primarily in the liver, and induces easily detectable changes in the *in vivo* ^{31}P MR liver spectrum. This observation has raised the hope that the dynamic ^{31}P MRS measurement of hepatic fructose metabolism may be valuable in evaluating liver function reserve both in animal models and in human patients.

The hepatic response to fructose loading has been intensively studied by various research groups using a variety of techniques. The metabolite concentrations in perfused rat liver before and after fructose administration have been assayed using chemical and enzymatic methods (6, 7). Many studies have used *in vitro* NMR methods with freeze-clamped liver extracts or *in vivo* NMR methods with perfused liver systems to investigate fructose-induced hepatic responses (8–10). During the last several years, noninvasive *in vivo* ^{31}P MRS with intact living animals or humans has been employed in the study of hepatic response to a fructose challenge (3, 9, 11–13). Most of these studies have monitored the response to fructose loading within healthy subjects. A few have reported the results from subjects with various types of hepatic failure, induced by portacaval shunt or due to clinical cirrhosis (12, 14, 15). In almost every study, from healthy or liver-damaged subjects, fructose induces an increase in the PME resonance as it is phosphorylated to fructose 1-phosphate (F1P), a decrease in ATP, the phosphate donor, and a decrease in P_i to replenish the ATP pool (8, 11, 12, 16, 17).

There have been virtually no studies of the liver's ability to metabolize a fructose load during an acute sublethal hepatotoxic challenge. Two classic model hepatotoxic compounds, carbon tetrachloride (CCl_4) and bromobenzene (BB), induce liver damage mainly by being metabolized to toxic free radicals (18–21), although covalent binding of reactive non-free radical intermediates may also contribute to tissue damage (22, 23). Various compounds can modulate their toxicity. Trolox C, a water soluble vitamin E analogue that scavenges free radicals, can protect the liver from free radical damage (21, 24, 25). Phenobarbital pretreatment induces increased metabolism of CCl_4 and BB to their toxic intermediates and increases the toxicity of these compounds (26).

We wanted to study the ability of an hepatotoxicant-challenged liver *in situ* to metabolize a fructose load. In this study, we determined a low dose of fructose that would *not* induce appreciable *in vivo* ^{31}P MR liver spectral changes in control rats. The hepatic response to this low fructose dose was then studied after an acute sublethal dose of CCl_4 or BB. Rats given fructose during an hepatotoxic insult showed a dramatic fructose-induced increase in hepatic PME not seen in controls, indicating

MRM 31:469–481 (1994)

From the Department of Chemistry and Biochemistry, University of Guelph, Guelph, Ontario, Canada.

Address correspondence to: Manfred Brauer, Ph.D., Department of Chemistry and Biochemistry, University of Guelph, Guelph, Ontario, Canada N1G 2W1.

Received June 29, 1993; revised November 30, 1993; accepted January 13, 1994.

This study was supported by the University of Guelph MRI facility and NSERC.

0740-3194/94 $3.00

altered liver function. For BB-treated rats, the fructose response was also studied after the liver had time to repair itself. The possible preventative effects of Trolox C and exacerbating effects of phenobarbital were also assessed in this study. *In vitro* ^{31}P MRS studies of perchloric acid extracts of livers freeze-clamped during fructose loading were used to further characterize the PME accumulation and bioenergetic changes during fructose loading. In addition, liver aldolase activities of controls and various treatment groups were measured to find out whether the hepatic accumulation of PME after fructose loading correlated with inhibition of liver aldolase activity. The results indicate that liver aldolase activity plays a key role in determining the amount of PME accumulation after a fructose challenge, and that aldolase activity is sensitive to hepatotoxic insult.

METHODS AND MATERIALS

Following a 12-h fast, male Wistar rats (250–350g) were given the following treatments. One group was given two doses of CCl_4 (160 µl/kg body weight) intraperitoneally, as an aqueous solution with 0.9% saline and 2% Myrj 45 emulsifier, 1 h apart. The second group was given 10 mmoles BB/kg body weight, intraperitoneally, as a 40% aqueous emulsion with 0.9% saline and 2% Myrj 45. The third group received not only the CCl_4 or the BB treatment as described above, but also a 5% (w/v) solution of Trolox C in propylene glycol (270 µmol/kg body weight, intraperitoneally) immediately after the CCl_4 treatment, or 1, 11, and 23 h after the BB treatment. A fourth group of rats was pretreated with phenobarbital before the BB treatment. Phenobarbital was administered to the rats as a 0.1% solution, which replaced the drinking water for 5 days prior to the treatment with BB (26). The BB dosage for this group of rats was 5 mmol/kg body weight, given intraperitoneally. Control rats received the same Myrj 45 emulsion without CCl_4 or BB.

CCl_4 and BB have previously been shown to induce hepatotoxicity under our experimental conditions. We have seen via MRI, the development of edema and via MRS, hepatic acidosis occurring from 2 to 14 h after administration of CCl_4 (27). BB is slower acting, and we have observed hepatic edema via MRI and changes in PME and ATP levels via MRS 12 to 48 h after BB administration (28). The dosages used for CCl_4 and BB are 50% of their LD_{50} values for rats (20–23). We have observed the same histological effects and increased levels of serum transaminases after hepatotoxicant administration as previously reported by other workers (21, 22, 27, 28).

All of the above rats received fructose at a dosage of either 7 mmol/kg body weight or 20 mmol/kg body weight, intraperitoneally (50% fructose in 0.9% saline). Fructose was given to the treated rats 4 or 9 h after the CCl_4 treatment, or 24, 48, and 120 h after the BB treatment. Each rat received only 1 dose of fructose. *In vivo* ^{31}P MR liver spectra were acquired immediately before fructose loading and every 12 min after administration of the fructose load. The fructose load was administered remotely via a syringe outside the magnet through thin tubing into the peritoneal cavity of the rat positioned inside the magnet. All rats were anesthetized before and during the fructose loading experiments with 1.5–2.0% isoflurane in 98% O_2 (1 l/min).

All the MRS experiments described in this study were performed on a Spectroscopy Imaging System (SISCO) 85/310 spectrometer (Fremont, California) at a magnetic field strength of 2.0 Tesla with a 31-cm horizontal bore magnet. *In vivo* ^{31}P MR spectra of rat livers were obtained without surgical intervention using a simple 2.0-cm (outer diameter) surface coil. To improve volume selection, the MRS signals from skin and muscle were reduced using an immobilized ferrite screen that induces B_0 field inhomogeneity in the region of the skin (29). T_1 effects were minimized by acquiring the spectra with a repetition time of 5.6 seconds. Control experiments showed that all resonances were over 90% of their fully relaxed intensities at 5.6 s relative to a repetition time of 10 s.

A sealed capillary of 0.1 *M* phosphonitrilic chloride (PNC) with 16 m*M* Cr(III) acetylacetonate in CCl_4 mounted 1.5 cm above the center of the surface coil was used as a signal intensity and radiofrequency pulse width standard (29). All spectra were acquired with the PNC capillary subjected to 90° pulses to obtain reproducible radiofrequency penetration into the animal. Data processing involved line broadening of 10 Hz and removal of resonances broadened by the ferrite screen from *in vivo* ^{31}P liver spectra by convolution difference methods (10–200 Hz line-broadening). The resonance areas and peak heights were normalized relative to the PNC resonance to account for variations in surface coil sensitivity between experiments. Data analysis was conducted on resonance integrals using a spectral simulation program (SISCO deconvolution line-shape analysis) (28, 29). Only initial estimates of chemical shifts were given as starting points for the iterative curve-fitting procedure.

The pH values were derived from the chemical shift of the observed *in vivo* P_i resonance. The Henderson-Hasselbach relationship was used: $pH = 6.75 + \log[(\delta - 0.75)/(3.35 - \delta)]$, where δ is the chemical shift in ppm for the *in vivo* P_i resonance (29, 30). All chemical shifts are given relative to 85% phosphoric acid (external sample). The relatively pH-insensitive resonance for the α-phosphate of ATP was used as an internal chemical shift reference.

In vitro ^{31}P MR spectra of perchloric acid (PCA) extracts of whole rat livers were obtained after the rats had been anesthetized with 1.5–2.0% isoflurane in 1 liter/min O_2, and the livers freeze-clamped and extracted with 6% PCA (31). Extracts were analyzed by conventional high resolution ^{31}P MRS on a Varian Unity 400 NMR spectrometer (Palo Alto, California), and were analyzed using our own previously published methods (31). Fructose 1-phosphate (F1P), adenosine- and inosine-monophosphate (AMP and IMP), α-glycerophosphate (αGP), fructose 1,6-diphosphate (FDP), glyceraldehyde 3-phosphate (GAP), and dihydroxyacetone phosphate (DHAP) resonances were identified by the increase in resonance intensities upon sequential addition of the pure compounds into liver PCA extracts.

Rat liver aldolase (ALD, EC 4.1.2.13) activity was measured as described by Nicholls *et al.* (32). The liver was homogenized with 12 to 15 passes of a Teflon pestle in 1 m*M* EDTA and 1 m*M* 2-mercaptoethanol, pH 7.0, and centrifuged at 3000 × *g* for 20 min at 4°C. The resultant supernatant fluid was centrifuged at 10,000 × *g* for 20 min, and the resultant clear supernatant fluid was frozen at −20°C with acetone-dry ice or used immediately for determining the enzyme activity. The aldolase was assayed using reagent kits obtained from the Sigma Chemical Co., St. Louis, MO. Enzyme units of rat liver aldolase activity were converted from SIGMA units to μmol/mg protein/h using the assumption that 1 g wet weight of rat liver tissue contains 140 mg protein (33).

Statistical analysis for the ^{31}P MRS changes between the various treatment groups as a function of time after fructose loading were performed using two-way analysis of variance (ANOVA) to find out whether the differences were significant in terms of treatment and time. The aldolase activity results from different groups of rats with different treatments were compared using the Student *t*-test.

The experimental protocol followed the guideline of the Canadian Council on Animal Care that has been approved by the local Animal Care Committee.

RESULTS

Figure 1 shows the *in vivo* ^{31}P MR liver spectra obtained from control rats immediately before, and 25 and 114 min after fructose loading (left to right), at two different fructose concentrations. It has been frequently reported that after fructose loading, a detectable increase in the PME resonance can be observed with healthy controls (3, 6, 8, 34, 35). In our studies, 20 mmole/kg body weight of fructose was given to control rats, as a intraperitoneal injection, and indeed a PME accumulation was observed (Fig. 1b). The fructose dosage was then reduced to levels that would not induce any detectable PME accumulation after fructose loading to the healthy control rats. It was found that with a fructose dosage of 7 mmol/kg body weight, no significant PME accumulation could be observed from the control rats after fructose loading (Fig. 1a). In all subsequent studies, the fructose responses of rats with hepatic failure caused by CCl_4 or BB treatment were studied at the fructose dosage of 7 mmol/kg body weight.

Figure 2 shows the *in vivo* ^{31}P MR liver spectra obtained from control (a), CCl_4-treated (c), and CCl_4 plus Trolox C-treated (b) rats immediately before fructose, and 25 and 114 min after fructose loading. Fructose was given to the treated rats 9 h after the CCl_4 treatment. At this 7 mmol fructose/kg body weight dosage, the three spectra of a typical control rat before fructose loading, and 25 and 114 min after fructose loading (Fig. 2a) are very similar: the prefructose PME signal was not high, the PME resonance increased very little 25 min after fructose loading, and the spectrum was almost identical with the prefructose spectrum 114 min after fructose loading. For a typical CCl_4-treated rat, in which fructose was given 9 h after the CCl_4 treatment (Fig. 2c), a significant PME accumulation could be observed 25 min after fructose loading. At the same time the P_i resonance decreased and a slight upfield shift in the P_i resonance position could be observed. For the spectral set recorded for a typical CCl_4 plus Trolox

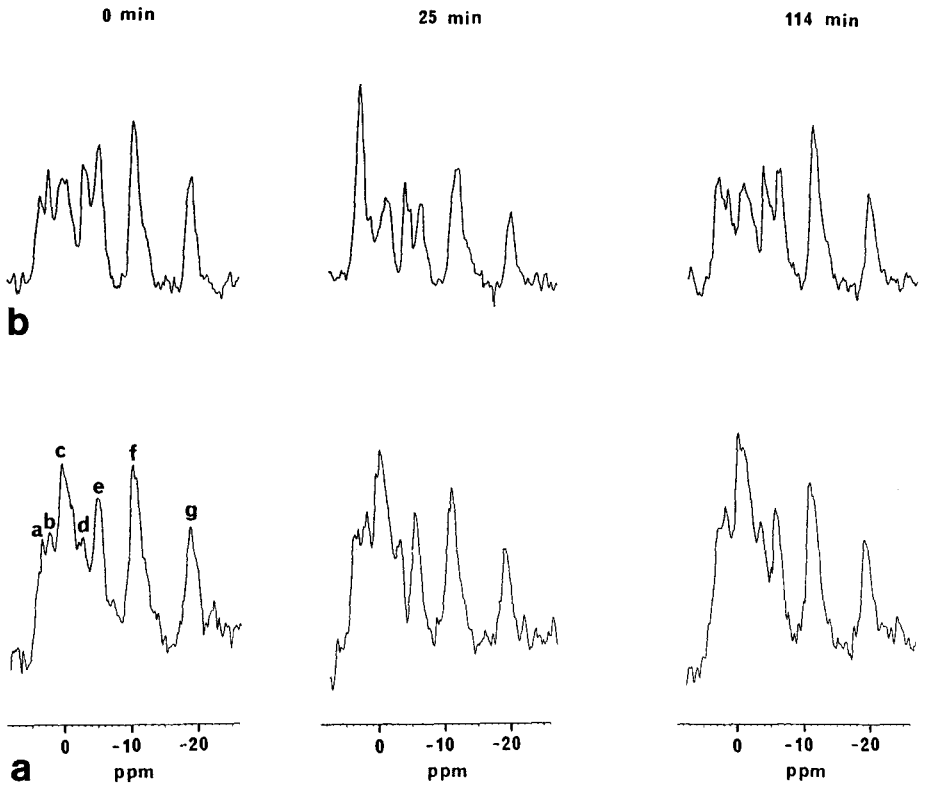

FIG. 1. In vivo ^{31}P MR spectra of livers of control rats receiving: (a) 7 mmol/kg body weight fructose (bottom row); and (b) 20 mmol/kg body weight fructose (top row) immediately before, and 25 and 114 min after an intraperitoneal injection of 50% fructose (left to right). The ^{31}P resonance assignments (Fig. 1a, t = 0 min) are as follows: (a) PME, (b) P_i, (c) PDE, (d) PCr, (e) γ phosphate, (f) α phosphate, and (g) β phosphate of ATP and other nucleotides.

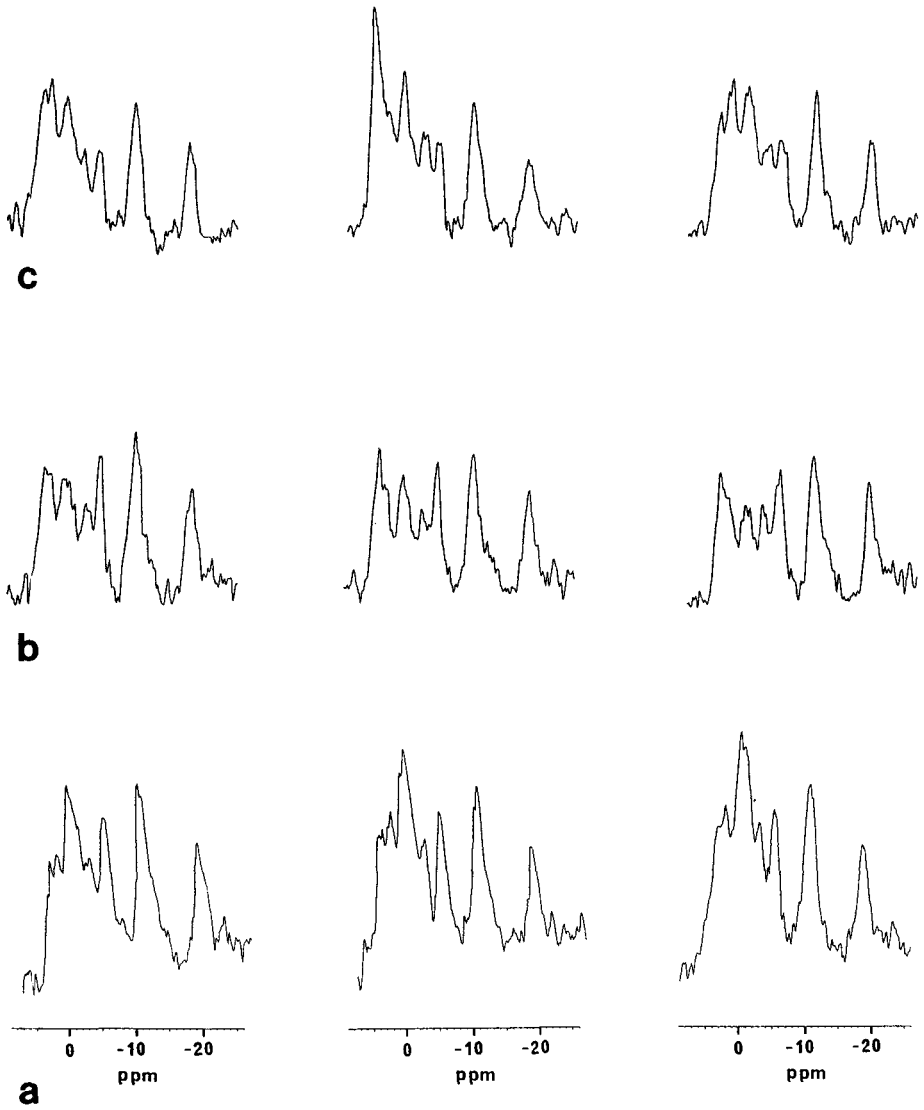

FIG. 2. *In vivo* ^{31}P MR spectra of livers of: (a) control rats (bottom row), (b) CCl_4 plus Trolox C-treated rats (middle row), and (c) CCl_4-treated rats (top row) immediately before, and 25 and 114 min after an intraperitoneal injection of 50% fructose (7 mmol/kg body weight). Fructose was administered to the treated rats 9 h after the CCl_4 treatment.

C-treated rat (Fig. 2b), the PME accumulation after fructose loading was not as great as with the CCl_4 treatment alone.

Figures 3a–3c show the average PME, ATP (β phosphate), and P_i resonance changes after fructose loading to control rats, CCl_4 9-h rats, and CCl_4 plus Trolox C-treated rats, as a percentage of the prefructose resonances. The mean ± standard error for each treatment group are indicated (n = 4 for controls, n = 3 for CCl_4, and CCl_4 plus Trolox C-treated groups). For the CCl_4-treated rats, the PME resonance increased to 155% of prefructose levels 25 min after fructose loading, and then started dropping between 25 and 63 min, and returned to its prefructose level. The PME level of the control rats did not change appreciably during the whole time course. A slight PME accumulation was observed for the CCl_4 plus Trolox C-treated rats. The ATP level decreased to 70–80% of the prefructose levels for the CCl_4-treated rats. The P_i level also appeared to decrease but accurate resonance integration was not possible, because of appreciable spectral overlap from the PME and PDE. No significant changes in the P_i resonance and the ATP resonance were found for the control and the CCl_4 plus Trolox C rats.

Figure 3d shows the intracellular pH changes for the control, the CCl_4 9-h, and the CCl_4 plus Trolox C rats during the study. Again, accurate chemical shift determination for the P_i resonance (and hence intracellular pH) is difficult, because the P_i resonance is not always resolvable. The hepatic pH of the control and the CCl_4 plus Trolox C rats did not change substantially during the time course with a pH value of around 7.3. For the CCl_4 9-h rats, there are two interesting points. First, the prefructose pH of the CCl_4 9-h rats was lower than that of the controls, with a value of about 7.15. Secondly, the pH of the CCl_4 9-h rats dropped to 6.8 from 7.15, 25 min after fructose loading, and recovered in the later stages to pH 7.1 to 7.2. Thus, the CCl_4 treatment induced an acidosis without fructose loading, as has been previously reported (27), and after fructose loading, the CCl_4-treated rats exhibited an additional drop in intracellular pH, not found for the control or the CCl_4 plus Trolox C-treated rats.

Similar experiments were also conducted with the CCl_4 4-h rats (spectra not shown). The PME accumulation was again readily detectable, but the depletion of P_i and ATP and the decrease in pH were less apparent than in the CCl_4 9-h rats as described above.

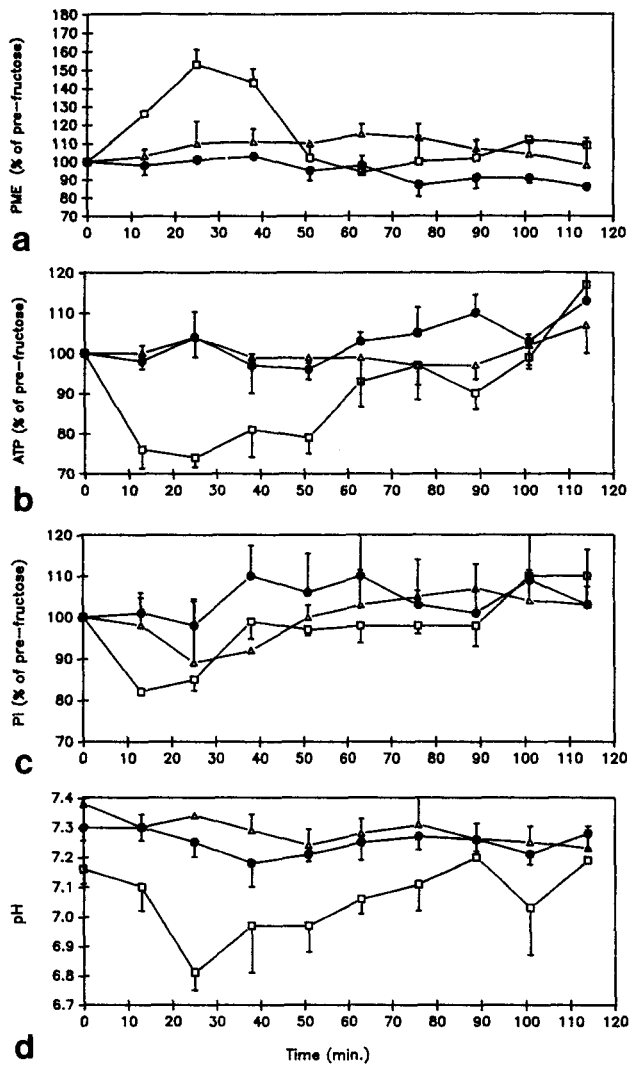

FIG. 3. Changes in the *in vivo* resonance of: (a) PME, (b) β-ATP, (c) P_i, and (d) changes in hepatic pH, for the control (solid circles), the CCl_4 treated (open squares), and the CCl_4 plus Trolox C-treated (open triangles) rat livers after fructose loading. Fructose was administered to the treated rats 9 h after the CCl_4 treatment. Each data point represents the mean ± standard error for three (treated) or four (control) rats. In Figs. 3a–3c, changes are expressed as percentages relative to the spectra immediately before fructose loading.

Figure 4 shows the *in vivo* ^{31}P MR liver spectra obtained from control (a), BB-treated (c), and BB plus Trolox C-treated (b) rats immediately before fructose, and 25 and 114 min after fructose loading. Fructose was given to the treated rats 24 h after the BB treatment. The prefructose PME level of the BB 24-h rats was already substantially higher than that of controls (Fig. 4c). This higher prefructose PME signal intensity has been previously reported to be due to BB-induced hepatic damage resulting in a dramatic and selective increase in phosphocholine (28, 29). The PME resonance increased even more after fructose loading. The prefructose PME of the BB 24-h plus Trolox C rats (Fig. 4b) was higher than that of the control as with the BB 24-h rats. However, after fructose loading, the PME accumulation of the BB 24-h plus Trolox C rats was not as marked as with the rats treated with only BB. Thus, Trolox C could not prevent the increase in the prefructose PME caused by BB treatment, but could suppress the subsequent PME accumulation caused by fructose loading.

Figure 5 shows the average PME, ATP, and P_i resonance changes as a percentage of the prefructose resonances after fructose loading to control rats, BB 24-h rats, and BB plus Trolox C-treated rats (each data point is a mean ± SE, $n = 4$ for controls, $n = 6$ for BB-treated rats, and $n = 3$ for BB plus Trolox C-treated rats). For BB-treated rats, the PME resonance increased from 13 to 38 min after fructose administration, reaching 190% of the prefructose level (Fig. 5a). The ATP levels (Fig. 5b) first decreased to 70% of the prefructose level and then came back to prefructose levels 50 min after fructose loading. The P_i resonance intensity for the BB-treated rats (Fig. 5c) was difficult to determine accurately, but appeared to decrease to about 70% of the prefructose level 13 min after fructose loading, and generally remained below control P_i levels over the 120-min time course. (Because of the large PME resonance in the BB-treated rats, it was difficult to resolve the P_i resonance and hence intracellular pH values could not be accurately determined). For BB plus Trolox C-treated rats after fructose loading, the degree of PME increase, ATP decrease, and P_i decrease was more moderate compared with BB-treated rats.

The PME resonance intensity changes with time as a percentage of the prefructose levels were plotted in Fig. 6 for BB 24-h (a), BB 48-h (b), BB 120-h (c), and the phenobarbital-pretreated rats (d). BB-induced liver damage is maximal at 24 to 48 h, while at 120 h, other observed manifestations of liver damage, such as elevated transaminase levels, and MRI-detected edema, have subsided (23, 28) and liver repair is well under way. The fructose-induced PME resonance increase was also greatest 24 to 48 h after BB treatment (Figs. 6a and 6b). The rats responded to fructose loading in a way similar to controls 120 h after the BB treatment, likely indicating a return of liver function to normal. Phenobarbital pretreatment induces the cytochrome P-450 system resulting in increased hepatotoxicity of BB, even at one-half the normal BB dosage (23). This is reflected in the dynamic ^{31}P MRS response of the phenobarbital pretreated rats (Fig. 6d).

Two-way ANOVA was used to find out whether the treatments (CCl_4 or BB, with or without Trolox C) had a statistically significant effect on the PME, ATP, P_i, or intracellular pH and whether the metabolite levels changed significantly with time. The results are summarized in Table 1. The PME, P_i, ATP, and pH changes were significantly different between the CCl_4 (4-h and 9-h) or BB-treated (24-h) rats and the controls. On the other hand, the pH changes for both BB plus Trolox C and CCl_4 9-h plus Trolox C rats were not significantly different from those of the controls. In addition, the P_i and ATP changes for the CCl_4 9-h plus Trolox C compared with controls were not significant. These results show that Trolox C did reduce the hepatic damage caused by CCl_4 or BB treatment.

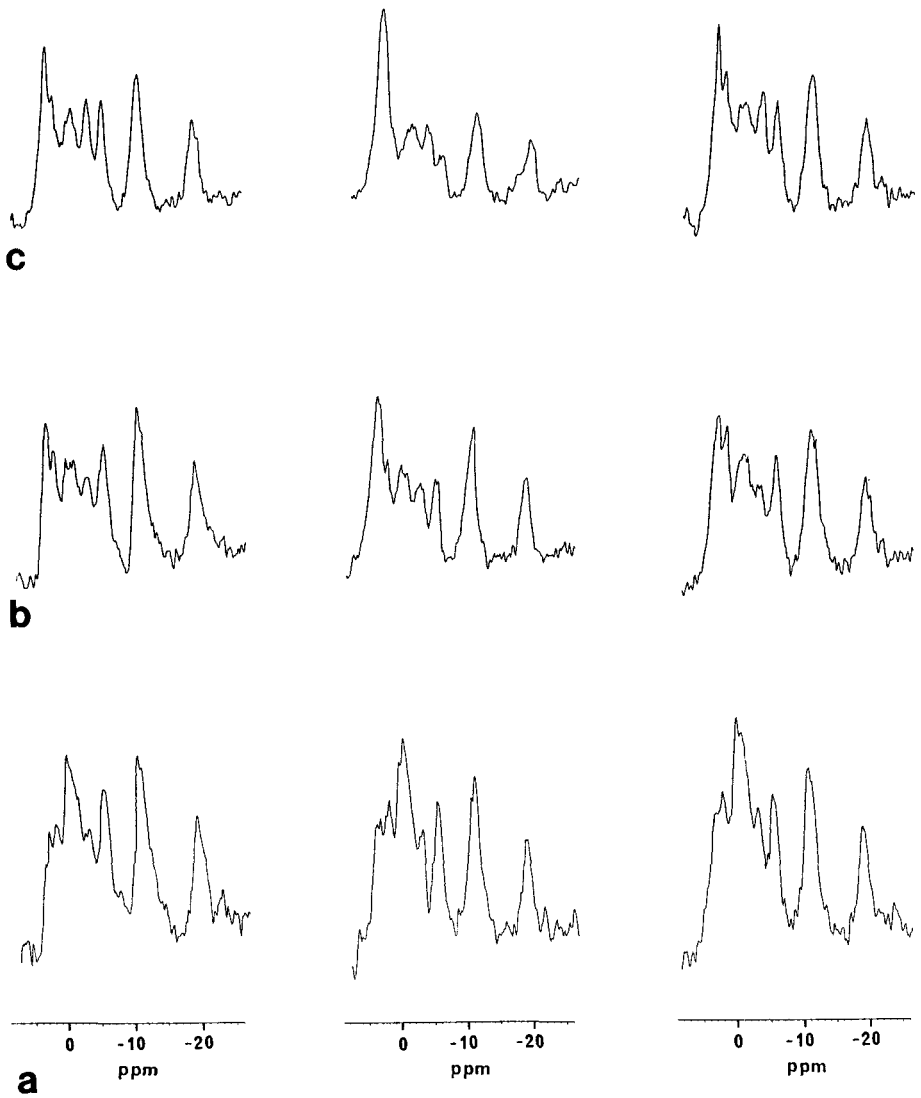

FIG. 4. *In vivo* ^{31}P MR spectra of livers of: (a) control rats (bottom row), (b) BB plus Trolox C-treated rats (middle row), and (c) BB-treated rat (top row) immediately before, and 25 and 114 min after an intraperitoneal injection of 50% fructose (7 mmol/kg body weight). Fructose was administered to the treated rats 24 h after the BB treatment.

Figure 7 shows the *in vitro* ^{31}P MR spectra of PCA liver extracts for a typical set of rats. Figures 7a and 7b show the *in vitro* ^{31}P MR spectra of PCA liver extracts from a typical control rat liver (Fig. 7a) and a rat liver 9 h after CCl_4 treatment (Fig. 7b), both without fructose loading. Figure 7c shows the *in vitro* ^{31}P MR spectrum of a PCA liver extract from a rat 9 h after the CCl_4 treatment, and 25 min after a 7-mmol/kg body weight (intraperitoneal) dose of fructose was given. Figures 7d–7f show expansions of the PME region of Figs. 7a–7c, respectively. The resonance assignments are listed in Table 2, and average metabolite concentrations (n = 3 rats for each treatment group) determined from the *in vitro* MR spectra are shown in Table 3. Comparing the results from CCl_4 9-h rats before fructose loading to the results from CCl_4 9-h rats 25 min after fructose loading, several increased PME resonances could be observed. From Table 3, we can see that fructose 1-phosphate (F1P) increased 12-fold, glucose 6-phosphate (G6P) increased threefold, fructose 1,6-diphosphate (FDP) increased 1.7-fold, α-glycerophosphate (αGP) increased twofold, and glyceraldehyde 3-phosphate (GAP) increased from undetectable levels to 0.42 μmol/g of wet liver. Adding up all the PME metabolite concentrations, the total PME concentration 25 min after fructose loading was 140% of the prefructose PME concentrations, correlating well with the *in vivo* results in which a 155% increase in the PME level was found (Fig. 3a). About 70% of the increase in PME after fructose loading was due to an increase in F1P (Table 3). For the *in vitro* MRS results, the ATP concentration decreased to 70% of prefructose levels after fructose loading and no significant change in P_i concentration was found. Comparing the results from control rats with rats treated with CCl_4 (9 h after CCl_4 treatment, no fructose loading), a 2.7-fold increase in phosphocholine resonance was found for the treated rats. This CCl_4-induced increase in phosphocholine has been previously reported (27).

Table 4 summarizes the aldolase activities measured from rat livers following the various toxicological treatments already studied. The control rats have the highest aldolase activities (around 4.8 enzyme units), and the CCl_4 9-h and BB 24-h rats have the lowest aldolase activity (2.5–2.6 enzyme units, 55% of the controls), with the aldolase activities of the CCl_4 9-h plus Trolox C, BB 24-h plus Trolox C, CCl_4 4-h, and BB 120-h rats in-between. The Student t-test results, also included in Table 4, show the

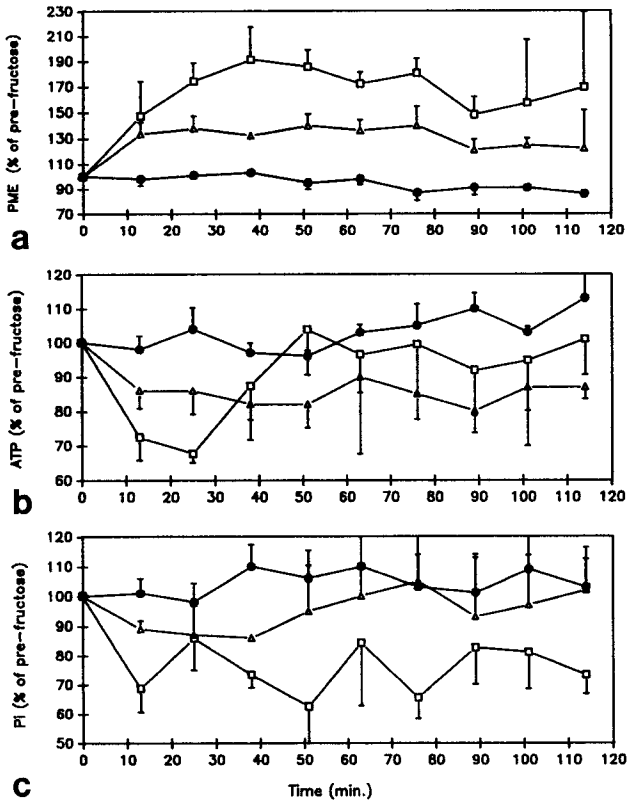

FIG. 5. Changes in the *in vivo* resonances of: (a) PME, (b) β-ATP, and (c) P_i resonances of the control (solid circles), the BB-treated (open squares), and BB plus Trolox C-treated (open triangles) rat livers after fructose loading. Fructose was administered to the treated rats 24 h after the BB treatment. Each data point represents the mean ± standard error (n = 4 for controls, n = *6* for BB-treated rats, and n = 3 for BB plus Trolox C-treated rats). Changes are expressed as percentages relative to the spectra immediately before fructose loading.

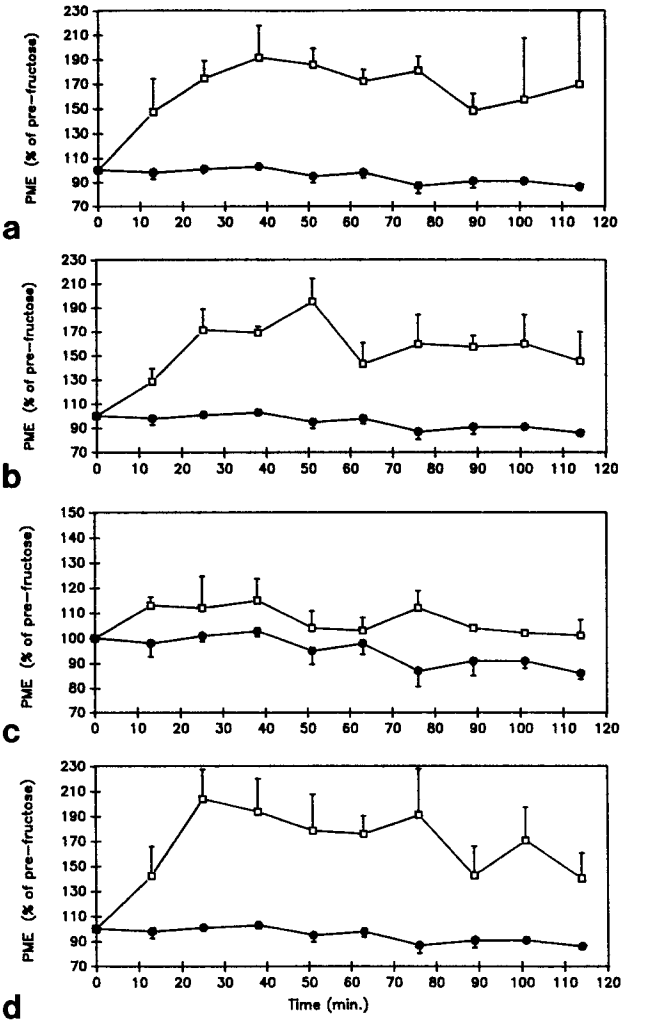

FIG. 6. Changes in the *in vivo* PME resonance of control (solid circles) and BB-treated (open squares) rat livers. Fructose 7 mmol/kg body weight, was administered: (a) 24 h, (b) 48 h, and (c) 120 h after the BB treatment, (10 mmol/kg BB). The treatment group in Fig. 6d was pretreated with phenobarbital before the BB treatment (24 h), and the BB dosage was 5 mmol/kg body weight. Each data point represents the mean ± standard error (n = 4 for controls, n = 6 for BB 24 h rats, and n = 3 for BB 48 h, BB 120 h, and phenobarbital pretreated rats). Changes are expressed as percentages relative to the spectra immediately before fructose loading.

significant differences of aldolase activity between the controls and the toxicant-treated groups, and between the toxicant-treated and the toxicant plus Trolox C-treated groups. The aldolase activities for the various treatment groups in Table 4 were plotted relative to the maximum percent increase in PME determined from the dynamic *in vivo* ^{31}P MRS studies (Figs. 3, 5, and 6). The results shown in Fig. 8 indicate that fructose-induced increase in PME, i.e., F1P accumulation, is inversely related to liver aldolase activity, with a statistically significant correlation coefficient of −0.834 ($P < 0.05$).

DISCUSSION

The hepatic response to fructose loading has been extensively studied both by *in vitro* ^{31}P MRS of freeze-clamped PCA extracts of livers, and by *in vivo* ^{31}P MRS of perfused livers and livers *in situ* within intact living humans or animals. Various studies have investigated the mechanisms of ATP depletion, the decrease in the P_i resonance, and other effects (11, 16, 17). The most pronounced spectral change is the significant PME accumulation after fructose loading. However, the mechanism of PME accumulation has not been examined in detail, other than some early biochemical studies of perfused livers (6).

It has been accepted that the PME increase after fructose loading is mainly due to an increase of F1P. Wood *et al.* reported that for normal rat liver perfused in a medium containing 10 m*M* fructose, the F1P concentration increased 38-fold (from 0.23 μmol/g wet weight to 8.72 ± 0.83 μmol/g wet weight) 10 min after starting the perfusion (6). Thoma and Uğurbil reported high resolution *in vitro* MR spectra of the PCA extracts of livers perfused in a medium containing fructose, and found that a high F1P resonance existed in the PME region (10). We also measured the high resolution *in vitro* ^{31}P MR spectra of PCA

Table 1
Two-Way ANOVA Test of Treatment and Time Effects of Fructose Loading on *In Vivo* ^{31}P MR Liver Spectra[a]

Treatment	PME		β-ATP		P_i		pH	
	P (treat)	*P* (time)	*P* (treat)	*P* (time)	*P* (treat)	*P* (time)	*P* (treat)	*P* (time)
CCl_4 4-h vs. control	0.000	0.011	0.000	0.782 (n.s.)[b]	0.001	0.013	0.000	0.950 (n.s.)
CCl_4 9-h vs. control	0.000	0.000	0.000	0.000	0.005	0.000	0.000	0.004
BB 24-h vs. control	0.000	0.000	0.000	0.001	—[c]	—	—	—
BB 120-h vs. control	0.000	0.091 (n.s.)	0.805 (n.s.)	0.040	0.001	0.091 (n.s.)	0.000	0.189 (n.s.)
CCl_4 9-h-Trolox vs. control	0.000	0.018	0.744 (n.s.)	0.464 (n.s.)	0.168 (n.s.)	0.424 (n.s.)	0.254 (n.s.)	0.478 (n.s.)
BB 24-h Trolox vs. control	0.000	0.003	0.000	0.359 (n.s)	0.001	0.787 (n.s.)	0.526 (n.s.)	0.794 (n.s.)
CCl_4 9-h-Trolox vs. CCl_4 9h	0.001	0.000	0.000	0.000	0.053 (n.s.)	0.000	0.000	0.028
BB 24-h Trolox vs. BB 24h	0.016	0.000	0.004	0.000	—	—	—	—

[a] $n = 3$ for all treatment groups, $n = 4$ for control group.
[b] n.s., not significant.
[c] Could not be accurately determined due to resonance overlap.

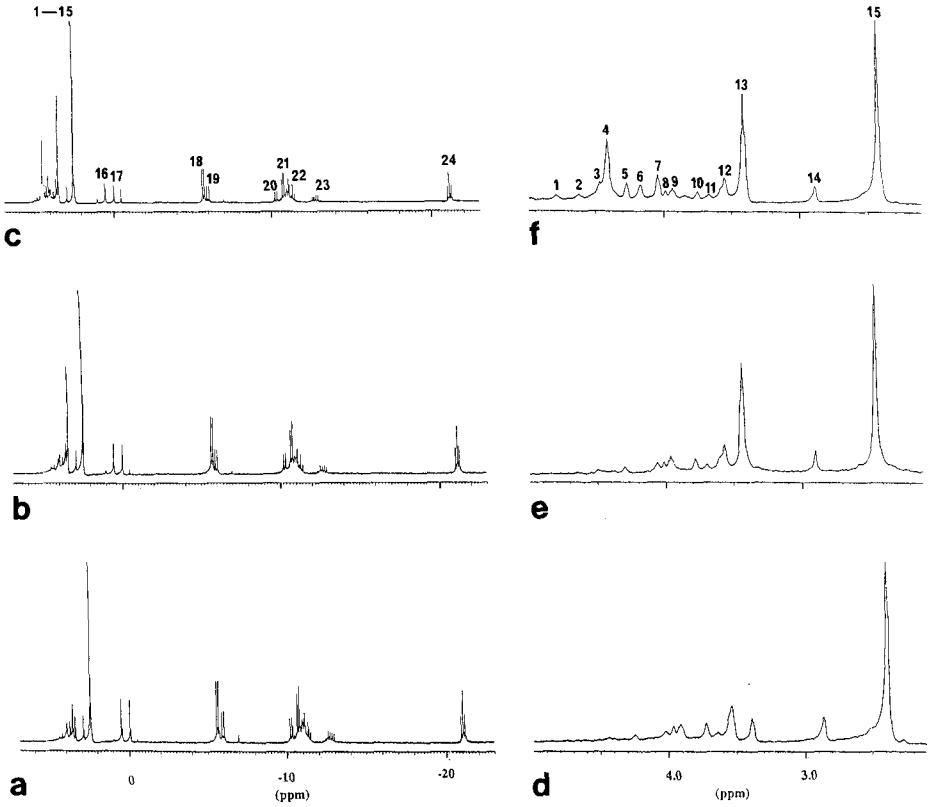

FIG. 7. *In vitro* ^{31}P MR spectra of PCA extracts of (a) control rat liver, not fructose loaded, (b) CCl_4 9-h rat liver, not fructose loaded, and (c) CCl_4 9-h rat liver, 25 min after fructose administration. The down-field region is expanded, and labeled as (d) for control without fructose loading, (e) for CCl_4 9-h rat without fructose loading, and (f) for CCl_4 9-h rat 25 min after fructose loading. The resonance assignments are listed in Table 2.

extracts of the rat livers after fructose was administrated to the rat, and found that the F1P resonance increased 12-fold compared with that of rats without fructose administration (Fig. 7). Approximately 70% of the increase in PMEs was due to this increase in F1P (Table 3). Other metabolites also increased after fructose loading, but not as dramatically as F1P. This indicates that steps subsequent to the aldolase-catalyzed breakdown of F1P proceed relatively quickly and do not result in appreciable accumulation of phosphorylated metabolites.

We have found that after low dose fructose loading (7 mmol/kg, given intraperitoneally), the PME resonance increases significantly for CCl_4 or BB-treated rats, the PME resonance increases less for rats treated with CCl_4 plus Trolox C or BB plus Trolox C, and the PME resonance does not increase significantly for healthy control rats. In addition, the CCl_4 or BB-treated rats have the lowest liver aldolase activity (≈2.5 enzyme units), the healthy control rats have the highest liver aldolase activity (around ≈4.8 enzyme units), and the liver aldolase activity of the rats treated with CCl_4 plus Trolox C or BB plus Trolox C was intermediate (≈3.4 enzyme units) (Table 4). Thus, the liver aldolase activity is inversely correlated ($r = -0.834$, $P < 0.05$) to the level of the PME accumulation after

Table 2
Resonance Assignments of a ^{31}P NMR Spectrum of the PCA Extract of Rat Liver from a CCl_4 9-h + Fructose Rat

Peak Number	Chemical Shift (ppm)[a]	Assignment	Abbreviation
1	4.80	Unknown 1	UN1
2	4.62	Unknown 2	UN2
3	4.47	Glucose 6-phosphate	G6P
4	4.41	Fructose 1-phosphate	F1P[2]
5	4.27	Glyceraldehyde 3-phosphate	GAP[2]
6	4.17	α-Glycerophosphate	αGP[2]
7	4.04	Fructose 1,6-diphosphate	FDP[2]
8	3.99	3-Phosphoglycerate	3PG
9	3.94	Phosphoethanolamine & dihydroxyacetone phosphate	PEth & DHAP
10	3.76	Adenosine monophosphate & inosine monophosphate	AMP & IMP[b]
11	3.67	Fructose 6-phosphate	F6P
12	3.55	P3, 2,3-Biphosphoglycerate	BPG(P-3)
13	3.41	Phosphocholine	PCh
14	2.89	P2, 2,3-Bisphosphoglycerate	BPG(P-2)
15	2.43	Inorganic phosphate	P_i
16	0.49	Glycerophosphoethanolamine	GPE
17	-0.06	Glycerophosphocholine	GPC
18	-5.67,-5.77	γ-P of ATP (doublet)	
19	-5.92,-6.06	β-P of ADP (doublet)	
20	-10.21,-10.34	α-P of ADP (doublet)	
21	-10.67,-10.79	α-P of ATP (doublet)	
22	-11.01,-11.31	Diphosphodiesters mainly NAD(H) and NADP(H)	DPDE1
23	-12.53,-12.91	Diphosphodiesters mainly UDP-glucose, etc.	DPDE2
24	-20.99,-21.11,-21.22	β-P of ATP (apparent triplet)	

[a] Relative to 85% H_3PO_4.
[b] Resonances identified by the increase in resonance intensities upon addition of pure compounds to liver PCA extracts. Other resonances were assigned according to a previous study (Ling and Brauer, 1990).

fructose loading (as shown in Fig. 8). The higher the liver aldolase activity is, the less PME (F1P) accumulates after fructose loading. This strongly suggests that the step in fructose metabolism that involves aldolase is the rate determining step.

Fructose is metabolized in the liver as:

$$\text{fructose} + \text{ATP} \xrightarrow{\text{fructokinase}} \text{F1P} + \text{ADP}$$

$$\text{F1P} \xrightarrow{\text{aldolase B}} \text{DHAP} + \text{D-glyceraldehyde}$$

Woods *et al.* proposed that aldolase is partially inhibited after fructose loading because of the increase in the concentration of IMP, an effective inhibitor of liver aldolase with a K_I of 0.1 m*M* (6). The accumulation of IMP is presumably due to the decrease in concentration of ATP and P_i after fructose loading, both of which are inhibitors of IMP formation from AMP. However, the role of IMP in regulating aldolase activity has been disputed (17), because fructose loading results in an increase in F1P *before* IMP levels rise. Brosnan *et al.* (13) reported an accumulation of PME in transgenic mouse liver but with no increase in IMP during fructose loading. In addition, our *in vitro* results (Fig. 7) show no increase in IMP or in AMP, the precursor for IMP, but rather a ≈30% decrease in the resonance of AMP+IMP for the CCl_4 treated rats after fructose loading. Because the K_I for IMP inhibition of aldolase B is relatively high (0.1 m*M*), and the concentration of AMP+IMP actually decreased from 0.43 to 0.29 μmole/g liver during fructose loading (Table 3), it is unlikely that IMP inhibits aldolase appreciably. Liver aldolase activity for the CCl_4 or BB-treated rats were lower than controls *before fructose loading*, suggesting that the inhibition of aldolase was not due to an increase in IMP as Woods proposed. Thus, the results presented in this study support the view that the PME accumulation after fructose loading is due to direct chemical modification inhibiting aldolase activity.

From what is known of the mechanisms of toxic action of CCl_4 and BB, it is not difficult to envisage how aldolase could be chemically modified and inactivated by reactive metabolites of these two hepatotoxicants. CCl_4 is reductively dehalogenated via the NADPH cytochrome P-450 mixed function oxidase system in the endoplasmic reticulum to form trichloromethyl radicals ($\bullet CCl_3$) and chloride anions (Cl^-). In the presence of oxygen, the $\bullet CCl_3$ radicals form trichloromethylperoxy radicals ($\bullet OOCCl_3$) that are thought to initiate a cascade of reactions, resulting in the peroxidative decomposition of membrane phospholipid fatty acids and subsequent breakdown in membrane integrity leading to hepatocellular necrosis (18–20). These reactive free radicals can also attack sensitive nucleophilic groups on enzymes such as cysteine thiols, histidine imidazoles, and serine hydroxyl groups. BB hepatotoxicity has two major toxic mechanisms of action–one is covalent binding of reactive epoxides and the other is free radical induced damage. BB is metabolized by the cytochrome P-450 system to one or more epoxides and liver injury is at least partially mediated by the covalent binding of the 3,4-epoxide to nucleophilic centers in essential target macromolecules (22, 23). The other important and perhaps dominant aspect of BB toxicity may be mediated

Table 3
Phosphorylated Metabolite Concentrations from *in Vitro* ^{31}P MRS Results[a]

Metabolites	CCl_4 9-h + fructose	CCl_4 9-h no fructose	Control no fructose	P[b] (CCl_4 9-h + Fructose vs. CCl_4 9-h)	P[b] (CCl_4 9-h vs. control)
UN1	0.22 ± 0.06				
UN2	0.26 ± 0.05				
G6P	0.54 ± 0.11	0.17 ± 0.04	0.14 ± 0.02	0.033[c]	0.549
F1P	1.55 ± 0.24	0.13 ± 0.03	0.12 ± 0.04	0.004[c]	0.798
GAP	0.42 ± 0.03				
αGP	0.45 ± 0.10	0.22 ± 0.01	0.23 ± 0.05	0.081	0.826
FDP	0.49 ± 0.08	0.29 ± 0.05	0.30 ± 0.07	0.096	0.914
3PG	0.22 ± 0.02	0.22 ± 0.01	0.23 ± 0.03	0.995	0.740
PEth + DHAP	0.39 ± 0.01	0.49 ± 0.04	0.42 ± 0.03	0.087	0.217
AMP + IMP	0.29 ± 0.05	0.43 ± 0.05	0.46 ± 0.05	0.105	0.666
F6P	0.30 ± 0.06	0.33 ± 0.06	0.23 ± 0.02	0.699	0.163
BPG(P3)	0.65 ± 0.08	0.81 ± 0.10	0.74 ± 0.17	0.287	0.721
PCh	2.03 ± 0.11	2.44 ± 0.30	0.59 ± 0.17	0.272	0.006[c]
BPG(P2)	0.35 ± 0.02	0.44 ± 0.05	0.60 ± 0.05	0.139	0.068
Pi	3.66 ± 0.22	3.45 ± 0.24	3.27 ± 0.17	0.553	0.563
GPE	0.64 ± 0.07	0.80 ± 0.08	1.20 ± 0.13	0.188	0.062
GPC	0.60 ± 0.06	0.66 ± 0.05	0.71 ± 0.09	0.442	0.647
γ-ATP	1.16 ± 0.19	1.68 ± 0.12	1.89 ± 0.05	0.082	0.172
β-ADP	0.49 ± 0.12	0.69 ± 0.04	0.73 ± 0.09	0.191	0.698
α-ADP	0.54 ± 0.10	0.99 ± 0.13	1.07 ± 0.22	0.055	0.774
α-ATP	1.38 ± 0.17	1.98 ± 0.13	2.20 ± 0.50	0.045[c]	0.700
DPDE1	2.28 ± 0.15	2.34 ± 0.10	2.56 ± 0.22	0.771	0.400
DPDE2	0.61 ± 0.07	0.58 ± 0.05	0.74 ± 0.11	0.779	0.260
β-ATP	0.99 ± 0.17	1.37 ± 0.09	1.55 ± 0.02	0.123	0.126

[a] n = 3 for all groups, concentration expressed as μmol/g of wet liver.
[b] Student's t test – P value.
[c] Significant ($P < 0.05$).

Table 4
Rat Liver Aldolase Activity

	Control	CCl_4 4-h	CCl_4 9-h	BB 24-h	BB 120-h	CCl_4 9-h + Trolox	BB 24-h + Trolox
Number of rats	12	5	3	3	4	7	6
Aldolase activity[a] ± standard error	4.76 ± 0.21	3.58 ± 0.23	2.56 ± 0.09	2.47 ± 0.04	3.26 ± 0.44	3.47 ± 0.19	3.29 ± 0.06
P of toxin treated vs. control[b]		0.005	0.000	0.000	0.004	0.001	0.000
P of toxin treated vs. toxin-Trolox treated[b]						0.008	0.000

[a] Unit of aldolase activity: μmol/mg protein/h.
[b] Student's t test.

through oxidative stress and free radical damage (36). Highly reactive O2• and H_2O_2 generated after BB administration, and free radical attack by $O_2^{\bullet}$ or H_2O_2 on unsaturated fatty acyl moieties of membrane phospholipids can initiate lipid peroxidation leading to damaged and leaky membranes. Because aldolase has several functional groups susceptible to attack by either reactive epoxides or free radicals, including an essential active site cysteine (37), the inactivation of aldolase by CCl_4 or BB metabolites can be readily accounted for. In addition, both CCl_4 and BB can deplete levels of reduced glutathione, that are necessary in preventing unwanted oxidized disulfide bridges in enzymes. It has been shown that depletion of reduced glutathione by itself can totally inhibit aldolase activity *in vivo* (38).

The magnitude of the hepatic PME accumulation after fructose loading is determined by the overall rate of the fructokinase step (formation of F1P) minus the overall rate of the aldolase step (breakdown of F1P). Because the first reaction has an *in vitro* V_{MAX} of 2.2 to 3.1 μmoles/min/g of tissue and the second reaction has an *in vitro* V_{MAX} of 1.6 to 3.4 μmoles/min/g of tissue (17), a 50% decrease in the aldolase activity could result in the large increase in net F1P accumulation that we have observed.

Besides the fructose-induced increase in PME, CCl_4 and BB decreased the bioenergetic reserve of the liver, so that a fructose load caused a detectable decrease in *in vivo* ATP and P_i levels and a decrease in intracellular pH *not* observed in controls (Figs. 3 and 5). The fructokinase reaction rapidly consumes ATP to phosphorylate the fructose load. For the toxicant-treated livers, the fructose-induced decrease in ATP and P_i reflects damage to the mitochondria reducing the rate of ATP resynthesis from ADP and intramitochondrial (i.e., NMR invisible) P_i. If the mitochondria cannot resynthesize ATP rapidly enough, the hepatocyte must rely on anaerobic glycolysis to make ATP, and more lactic acid will be produced decreasing the intracellular pH.

Trolox C, a water soluble vitamin E analogue, scavenges free radicals. Wu and coworkers have observed that

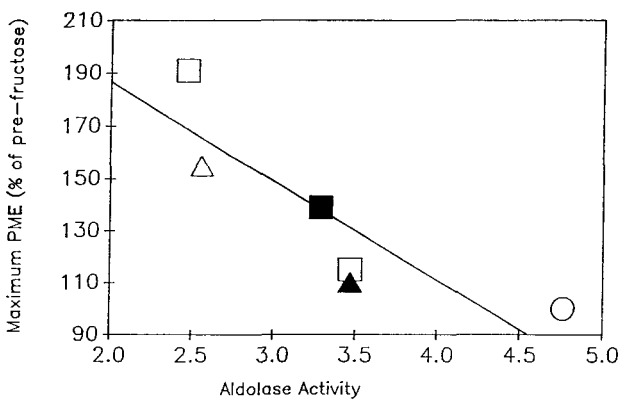

FIG. 8. Correlation of observed *in vivo* ^{31}P PME accumulation and liver aldolase activity. The maximum percent PME increase induced by fructose (Figs. 3, 5, and 6) is plotted relative to the liver aldolase activity for the same treatment group before fructose loading (Table 4). The correlation coefficient between PME accumulation and aldolase activity was –0.834, $P < 0.05$.

Trolox C protects human hepatocytes, myocytes, and erythrocytes against *in situ* generated oxyradicals (24, 25). The effects of Trolox C on BB hepatotoxicity *in vivo* have also been studied. The administration of Trolox C was found to almost completely prevent liver necrosis and lipid peroxidation due to free radical damage, while not affecting the extent of the covalent binding of BB metabolites (21). In our previous study (28), it has been shown that Trolox C could reduce the BB-induced hepatic edema and steady-state bioenergetic deterioration, although it does not prevent the BB-induced elevation in PME due to increased phosphocholine.

In this present study, it was found that both CCl_4 and BB treatments caused a decrease in liver aldolase activity. Trolox C protected the liver, ameliorating the decrease in liver aldolase activity. Therefore, the livers of Trolox C-treated rats could metabolize fructose more rapidly than CCl_4 or BB-treated rat livers, without as great a build-up of PME (F1P). Trolox C also prevented the decrease in ATP and P_i during fructose loading, indicating that the mitochondria are also protected. In addition, the prefructose hepatic acidosis caused by the CCl_4 treatment can be prevented by Trolox C, as well as the decrease in intracellular pH induced by the fructose challenge. These findings suggest that Trolox C preserves the capacity of the liver of the rats treated with CCl_4 and BB to metabolize a fructose load. The superior response to a fructose load for the rats treated with toxicant plus Trolox C simply reflects the increased hepatic function under Trolox C-induced protection from free radical attack. The observation that Trolox C cannot prevent the BB-induced prefructose PME elevation, but can reduce the PME elevation induced by fructose loading is because these two PME elevations are due to two different mechanisms. BB-induced prefructose PME elevation was found to be due to an increase in phosphocholine (28), while the latter is mainly due to an increase in F1P. The F1P elevation is influenced by aldolase activity, while the increase in phosphocholine is not related to this specific enzyme.

From the *in vitro* MRS results (Fig. 7 and Table 3), not only could the F1P increase be easily identified, but several other PME resonances were also found to increase after fructose loading. Figure 9 shows the basic metabolic pathways for fructose and glucose. After fructose loading, most of the fructose was metabolized through fructokinase to form F1P, and the accumulation of F1P had been discussed above. Similarly, a minor part of fructose is metabolized via hexokinase to fructose 6-phosphate, and then via phosphofructokinase to form FDP. The accumulation of FDP would be expected because of aldolase inhibition (aldolase B uses either F1P or FDP as a substrate). From the pathway, the increases in GAP and α-GP also can be explained, because these two metabolites are formed from the breakdown products of F1P and (to a lesser degree) FDP. It had been reported that fructose administration stimulates glucose phosphorylation in isolated hepatocytes (39–41), and in the livers of rats (41, 42). This effect has been explained by the property of F1P to relieve the inhibition that a regulatory protein exerts on glucokinase in the presence of F6P (42). From Fig. 7 and Table 3, a fourfold increase in G6P was observed. After fructose loading, both F1P and F6P were elevated in the hepatocytes. Thus, the increase in G6P can be explained as the result of stimulated glucose phosphorylation due to the products of fructose administration. Fructose-induced stimulation of glucose phosphorylation to G6P may explain the "glucose paradox" in which fructose, but not glucose alone, can ameliorate hypoxic liver injury (43).

It should be noted that our results agree with those involving some types of liver damage and disagree with others. For livers damaged via portacaval shunt (12), fructose infusion induced a higher PME build-up than in

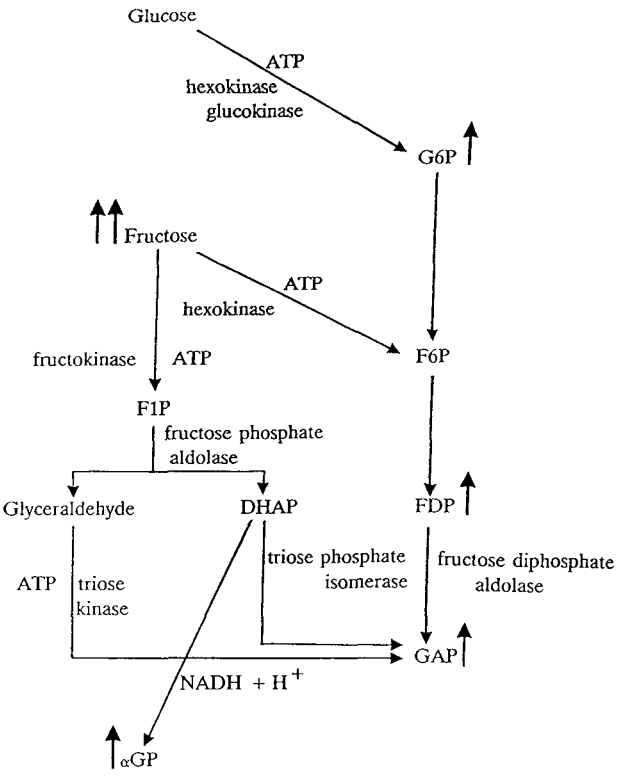

FIG. 9. Metabolic pathways for fructose and glucose in mammalian liver.

controls–as in our studies. However, clinical studies of patients with cirrhotic livers (15, 44) showed lower PME accumulation than controls. For chronic cirrhosis, hepatic blood flow is disrupted and the amount of functional liver has decreased and been replaced with metabolically inactive fibrotic scar tissue. In this case, fructose is not taken up very quickly by the residual active tissue, and little or no hepatic PME accumulation is detected (3, 44). Bates *et al.* (14) gave CCl_4 and acetaminophen to rats and found that the treated rats accumulated less PME than controls, in contrast to our studies. Bates *et al.* (14) used a fivefold higher dose of CCl_4 on the more susceptible phenobarbital pretreated rats, and did not test with fructose until 48 h after CCl_4 treatment. Their absolute metabolite intensities were considerably lower in the CCl_4 group than in controls, and they suggest that "there is a smaller functioning mass of cells than in the normal liver." By 48 h, their CCl_4 dose would be completely metabolized (21, 22), and the toxic metabolites would have killed most of the functional liver, leaving mainly inactive fibrotic tissue. Thus, as with the cirrhotic liver case, it appears that a smaller mass of functional liver can take up and phosphorylate less fructose and will result in a *lower* accumulation of PME. Conversely, a liver that is functionally impaired but still viable (under our experimental conditions, for example) and has not lost appreciable functional mass, will accumulate *more* PME after a fructose load. In view of the fact that PME buildup in a damaged liver after fructose loading may be either higher or lower than in controls, depending upon the extent and nature of the liver damage, the dynamic ^{31}P MRS fructose test by itself will not be a clinically useful test for the liver.

REFERENCES

1. D. I. Hoult, S. J. Busby, D. G Gadian, G. K. Radda, R. E. Richards, P. J. Seely, Observation of tissue metabolites using ^{31}P nuclear magnetic resonance. *Nature* **252,** 285–287 (1974).
2. S. M. Cohen, Physiological NMR spectroscopy: from isolated cells to man. *Ann. N. Y. Acad. Sci.* **508,** 1–498 (1987).
3. C. Segebarth, A. R. Grivegnee, R. Longo, P. R. Luyten, J. A. den Hollander, *In vivo* monitoring of fructose metabolism in the human liver by the means of ^{31}P magnetic resonance spectroscopy. *Biochimie* **73,** 105–108 (1991).
4. R. B. Moon, J. H. Richards, Determination of intracellular pH by ^{31}P magnetic resonance. *J. Biol. Chem.* **248,** 7276–7278 (1973).
5. M. J. Dawson, D. G. Gadian, D. R. Wilkie, Studies of skeletal muscle bioenergetics by ^{31}P NMR. *J. Physiol.* **267,** 703–735 (1977).
6. H. F. Woods, L. V. Eggleston, H. A. Krebs, The cause of hepatic accumulation of fructose 1-phosphate on fructose loading. *Biochem. J.* **119,** 501–510 (1970).
7. L. Sestoft, The cause of hepatic accumulation of fructose-1-phosphate on fructose loading. *Biochim. Biophys. Acta* **343,** 1–16 (1974).
8. R. A. Iles, J. R. Griffiths, A. N. Stevens, D. G. Gadian, Effects of fructose on the energy metabolism and acid-base status of the perfused starved rat liver. *Biochem. J.* **192,** 191–202 (1980).
9. R. A. Iles, A. N. Stevens, J. R. Griffiths, P. G. Morris, Phosphorylation status of liver by ^{31}P-NMR spectroscopy, and its implications for metabolic control. *Biochem. J.* **229,** 141–151 (1985).
10. W. J. Thoma, K. Uğurbil, Effect of adenine on liver nucleotide after fructose loading by ^{31}P-NMR. *Am. J. Physiol.* **256,** G949–G956 (1989).
11. G. S. Karczmar, T. Kurtz, N. J. Tavares, M. W. Weiner, Regulation of hepatic inorganic phosphate and ATP in response to fructose loading: an *in vivo* ^{31}P-NMR study. *Biochim. Biophys. Acta* **1012,** 121–127 (1989).
12. L. Rossaro, V. Mazzaferro, C. L. Scotti-Foglieni, D. Williams, E. Simplaceanu, V. Simplaceanu, A. Francavilla, T. E. Starzl, C. Ho, D. H. Van Thiel, Effect of cyclosporine on hepatic energy status and on fructose metabolism after portacaval shunt in dog as monitored by phosphorus-31 nuclear magnetic resonance spectroscopy *in vivo*. *Hepatology* **13,** 780–785 (1991).
13. M. J. Brosnan, L. Chen, C. E. Wheeler, T. A. Van Dyke, A. P. Koretsky, Phosphocreatine protects ATP from a fructose load in transgenic mouse liver expressing creatine kinase. *Am. J. Physiol.* **260,** C1191–C1200 (1991).
14. T. E. Bates, S. R. Williams, A. L. Basza, D. G. Gadian, E. A. Proctor, ^{31}P NMR study *in vivo* of metabolic abnormalities in rats with acute liver failure. *NMR Biomed.* **1,** 67–73 (1988).
15. H. Kato, S. Ebara, S. Watanabe, S. Kamiya, M. Ohto, M. Igarashi, H. Ikehira, T. Hashimoto, H. Hukuda, Y. Tateno, Chronic liver disease: standard P-31 spectroscopy and dynamic study after intravenous drip infusion of fructose. *Soc. Magn. Reson. Med.* **10,** 319 (1991). [Abstract]
16. R. C. Morris, Jr., K. Nigon, E. B. Reed, Evidence that the severity of depletion of inorganic phosphate determines the severity of the disturbance of adenine nucleotide metabolism in the rat liver and renal cortex of the fructose-loaded rat. *J. Clin. Invest.* **61,** 209–220 (1978).
17. G. Van den Berghe, The mechanism of ATP depletion in the liver after a load of fructose. *Curr. Top. Cell. Regul.* **13,** 98–128 (1978).
18. T. Slater, K. Cheeseman, K. U. Ingold, Free radical mechanisms in tissue damage. *Philos. Trans. R. Soc. Lond. [Biol.]* **B311,** 633–645 (1985).
19. R. O. Recknagel, E. A., Glende, Jr., A. M. Hruszkewycz, Chemical mechanisms in carbon tetrachloride toxicity, *in* "Free Radicals in Biology" (W. A. Pryor, Ed.), Vol. III, pp. 97–132, Academic Press, New York, 1977.
20. W. J. Brattin, E. Glende, Jr., R. O. Recknagel, Pathological mechanisms in carbon tetrachloride hepatotoxicity. *J. Free Radic. Biol. Med.* **1,** 27–38 (1985).
21. A. F. Casini, A. Pompella, M. Comporti, Mechanisms of cell injury in killing of cultured hepatocytes by bromobenzene. *Am. J. Pathol.* **118,** 225–237 (1985).
22. W. D. Reid, G. Krishna, Centrilobular hepatic necrosis related to covalent binding of metabolites of halogenated aromatic hydrocarbons. *Exp. Mol. Pathol.* **18,** 80–99 (1973).
23. T. J. Monks, S. S. Lau, Reactive intermediates and their toxicological significance. *Toxicology* **52,** 1–53 (1988).
24. T. W. Wu, N. Hashimoto, J. Wu, D. Carey, R. K. Li, D. Mickle, R. D. Weisel, The cytoprotective effect of Trolox demonstrated with three types of human cells. *Biochem. Cell Biol.* **68,** 1189–1194 (1990).
25. T. W. Wu, N. Hashimoto, X. Au, D. Carey, D. G. Mickle, J. Wu, Trolox protects rats hepatocytes against oxyradical damage and the ischemic rat liver from reperfusion injury. *Hepatology* **13,** 575–580 (1991).
26. S. Orrenius, Phenobarbital pre-treatment, further studies on the induction of the drug-hydroxylating enzyme system of liver microsomes. *J. Cell. Biol.* **26,** 725–733 (1965).
27. M. Brauer, R. A. Towner, I. Renaud, E. Janzen, D. L. Foxall, *In vivo* proton NMR imaging and spectroscopy studies of

halocarbon-induced liver damage. *Magn. Reson. Med.* **9,** 229–239 (1989).
28. S. J. Locke, M. Brauer, Response of rat liver *in situ* to Bromobenzene–*in vivo* proton MRI and ^{31}P MRS studies. *Toxicol. Appl. Pharmacol.* **110,** 416–428 (1991).
29. M. Brauer, S. J. Locke, Proton MRI and phosphorus-31 MRS studies of bromobenzene-induced liver damage in the rat. *Magn. Reson. Imaging* **10,** 257–267 (1992).
30. D. Rees, M. B. Smith, J. Harley, G. K. Radda, *In vivo* functioning of creatine phosphokinase in human forearm muscle, studied by ^{31}P NMR saturation transfer. *Magn. Reson. Med.* **9,** 39–52 (1989).
31. M. Ling, M. Brauer, *In vitro* ^{31}P NMR studies of rat liver subjected to chronic ethanol administration. *Biochim. Biophys. Acta* **1051,** 151–158 (1990).
32. D. M. Nicholls, K. Teichert-Kuliszewska, M. J. Kuliszwski, Kinetic analyses of rat liver aldolase activities. *J. Neurol. Sci.* **73,** 97–106 (1986).
33. R. Teschke, F. Moreno, A. S. Petrides, Hepatic microsomal ethanol oxidizing system: respective roles of ethanol and carbohydrates for the enhanced activity after chronic alcohol consumption. *Biochem. Pharmacol.* **30,** 1745–1751 (1981).
34. A. P. Koretsky, S. Wang, J. Murphy-Boesch, M. Klein, T. L. James, M. W. Weiner, ^{31}P NMR spectroscopy of rat organs, in situ, using chronically implanted radiofrequency coils. *Proc. Natl. Acad. Sci. (USA)* **80,** 7491–7495 (1983).
35. F. Terrier, P. Vock, J. Cotting, R. Ladebeck, J. Reichen, D. Hentschel, Effect of intravenous fructose on the P-31 MR spectrum of the liver: dose response in healthy volunteers. *Radiology* **171,** 557–563 (1989).
36. A. F. Casini, M. Giorli, R. J. Hyland, A. Serroni, D. Gilfor, J. L. Farber, Mechanisms of cell injury in the killing of cultured hepatocytes by bromobenzene. *J. Biol. Chem.* **257,** 6721–6728 (1982).
37. B. L. Horecker, O. Tsolas, C. Y. Lai, Aldolases, *in* "The Enzymes" (P. D. Boyer, Ed.), Vol. 7, pp. 213–258, Academic Press, New York, 1972.
38. M. J. McKay, J. S. Bond, Effects of oxidative stress and intracellular redox status on aldolase activity. *Prog. Clin. Biol. Res.* **180,** 351–361 (1985).
39. D. G. Clark, O. H. Filsell, D. L. Topping, Effects of fructose on hepatic glycolysis and gluconeogenesis rates. *Biochem J.* **184,** 501–507 (1979).
40. E. Van Schaftingen, A. Vandercammen, Stimulation of glucose phosphorylation by fructose in isolated rat hepatocytes. *Eur. J. Biochem.* **179,** 173–77 (1989).
41. D. R. Davies, M. Detheux, E. Van Schaftingen, Fructose 1-phosphate and the regulation of glucokinase activity in isolated hepatocytes. *Eur J. Biochem.* **179,** 173–177 (1990).
42. E. Van Schaftingen, Fructose administration stimulated glucose phosphorylation in the livers of anesthetized rats. *Eur. J. Biochem.* **179,** 179–184 (1989).
43. C. A. Brass, J. Crawford, J. Narciso, G. L. Gollan, Hypoxic liver injury and the ameliorating effects of fructose: the "glucose paradox" revisited. *J. Am. J. Physiol.* **263,** G293–300 (1992).
44. J-F. Dufour, C. Stoupis, F. Lazeyras, P. Vock, F. Terrier, J. Reichen, Alterations in hepatic fructose metabolism in cirrhotic patients demonstrated by dynamic ^{31}phosphorus spectroscopy. *J. Hepatol.* **15,** 835–842 (1992).